THE JOURNAL OF BIOLOGICAL CHEMISTRY VOL. 282, NO. 33, pp. 24407–24415, August 17, 2007

Catalase Takes Part in Rat Liver Mitochondria Oxidative Stress Defense*

Received for publication, February 22, 2007, and in revised form, April 24, 2007 Published, JBC Papers in Press, June 18, 2007, DOI 10.1074/jbc.M701589200

Mauro Salvi[‡], Valentina Battaglia[‡], Anna Maria Brunati[‡], Nicoletta La Rocca[§], Elena Tibaldi[‡], Paola Pietrangeli[¶], Lucia Marcocci[¶], Bruno Mondovì[¶], Carlo A. Rossi[‡], and Antonio Toninello[‡1]

From the [‡]Dipartimento di Chimica Biologica, Università di Padova, Viale G. Colombo 3, 35121 Padova, the [§]Dipartimento di Biologia, Università di Padova, Viale G. Colombo 3, 35131 Padova, and the [¶]Dipartimento di Scienze Biochimiche, A. Rossi Fanelli, Università di Roma "La Sapienza," P. le A. Moro 5, 00185 Roma, Italy

Highly purified rat liver mitochondria (RLM) when exposed to *tert*-butylhydroperoxide undergo matrix swelling, membrane potential collapse, and oxidation of glutathione and pyridine nucleotides, all events attributable to the induction of mitochondrial permeability transition. Instead, RLM, if treated with the same or higher amounts of H_2O_2 or tyramine, are insensitive or only partially sensitive, respectively, to mitochondrial permeability transition. In addition, the block of respiration by antimycin A added to RLM respiring in state 4 conditions, or the addition of H_2O_2, results in O_2 generation, which is blocked by the catalase inhibitors aminotriazole or KCN. In this regard, H_2O_2 decomposition yields molecular oxygen in a 2:1 stoichiometry, consistent with a catalatic mechanism with a rate constant of 0.0346 s^{-1}. The rate of H_2O_2 consumption is not influenced by respiratory substrates, succinate or glutamate-malate, nor by *N*-ethylmaleimide, suggesting that cytochrome *c* oxidase and the glutathione-glutathione peroxidase system are not significantly involved in this process. Instead, H_2O_2 consumption is considerably inhibited by KCN or aminotriazole, indicating activity by a hemoprotein. All these observations are compatible with the presence of endogenous heme-containing catalase with an activity of 825 ± 15 units, which contributes to mitochondrial protection against endogenous or exogenous H_2O_2. Mitochondrial catalase in liver most probably represents regulatory control of bioenergetic metabolism, but it may also be proposed for new therapeutic strategies against liver diseases. The constitutive presence of catalase inside mitochondria is demonstrated by several methodological approaches as follows: biochemical fractionating, proteinase K sensitivity, and immunogold electron microscopy on isolated RLM and whole rat liver tissue.

Many human diseases, including cancer and other pathologies associated with aging, such as arteriosclerosis and cataracts, are related to mitochondrial dysfunctions provoked by reactive oxygen species (ROS)[2] (1). In this regard, the so-called free radical theory of aging has been proposed (2). ROS are highly reactive and may be extremely toxic in biological systems, as they attack a variety of molecules, including proteins, polyunsaturated lipids, and nucleic acid (3), causing the cell to die by apoptosis or necrosis. In physiological conditions, 1–2% of molecular oxygen consumption during mitochondrial respiration undergoes incomplete reduction by single electrons to form superoxide anion ($O_2^{\cdot-}$) at the level of NADH-ubiquinone reductase (complex I) and ubiquinol-cytochrome *c* reductase (complex III). These two segments of the respiratory chain generate the superoxide radical by autoxidation of reduced flavin and by transferring an electron from reduced ubisemiquinone to molecular oxygen, respectively (4). Superoxide is rapidly converted to hydrogen peroxide by mitochondrial superoxide dismutase, which then produces the highly reactive hydroxyl radical ($OH^{\cdot}$) by interacting with transition metal ions (Fe^{2+}) of the respiratory complexes (Fenton reaction), unless H_2O_2 is removed by the action of glutathione peroxidase (Gpx) or catalase (see below).

In physiological conditions, the primary defense against superoxide anion and hydrogen peroxide in mitochondria not containing catalase is performed by the concerted action of the above mentioned superoxide dismutase and Gpx. However, despite the activity of these enzymes, significant amounts of H_2O_2 can diffuse out from mitochondria to cytosol, where detoxification occurs through cytosol Gpx or by peroxisome catalase. In pathological conditions, *e.g.* during inflammation, hyperoxia (5), or chemotherapy (6), *i.e.* in the presence of large amounts of ROS, catalase becomes the most important scavenger of H_2O_2 in the cytosol. These conditions may be even more serious in mitochondria, as also observed in "*in vitro*" investigations with the organelle treated with monoamines (7), flavones (8), isoflavones (9), and cyclic triterpenes (10, 11). By interacting with transition metals of the respiratory chain, these compounds produce H_2O_2 and the highly toxic hydroxyl radical. These species, besides causing peroxidation of the phospholipid bilayer, with consequent severe damage to membrane integrity (12), can also induce mitochondrial permeability transition (9–11, 13, 14) with release of cytochrome *c* and activation of the pro-apoptotic cascade. The presence of catalase is of great importance, as its scavenging of H_2O_2 protects these organelles against the above damaging effects (15). The prob-

* The costs of publication of this article were defrayed in part by the payment of page charges. This article must therefore be hereby marked "*advertisement*" in accordance with 18 U.S.C. Section 1734 solely to indicate this fact.

[1] To whom correspondence should be addressed: Dipartimento di Chimica Biologica, Università di Padova, Istituto di Neuroscienze del CNR, Viale G. Colombo 3, 35121 Padova, Italy. Tel.: 39-0498276134; Fax: 39-0498276133; E-mail: antonio.toninello@unipd.it.

[2] The abbreviations used are: ROS, reactive oxygen species; ATZ, aminotriazole; Gpx, glutathione peroxidase; NEM, *N*-ethylmaleimide; MAO, monoamine oxidase; MPT, mitochondrial permeability transition; PMCA, plasma membrane Ca^{2+}-ATPase; RLM, rat liver mitochondria; Tbh, *tert*-butylhydroperoxide; TNF-α, tumor necrosis factor-α; TPP^+, tetraphenylphosphonium.

lem of the presence of catalase in mitochondria was examined many years ago by Neubert *et al.* (16), but so far the presence of this enzyme has been clearly demonstrated only in rat heart mitochondria (17). More recently, it has been demonstrated that yeast catalase A, which contains two peroxisomal targeting signals, can also enter mitochondria, although the enzyme lacks a classical mitochondrial import sequence (18). The key role that a possible mitochondrial catalase may play in oxidant defense has been demonstrated by several research groups, by experimentally targeting catalase to mitochondria. In these studies, the introduction of catalase into mitochondria provides better protection than cytosol expression against H_2O_2-induced injury (19), oxidative damage, and mitochondrial DNA deletion, and in extending the murine life span (20). In light of the importance of these results and considering the general opinion that catalase is present only in heart mitochondria (15, 17), the aim of this study is to ascertain if catalase is constitutively present in the mitochondria of liver, a multifunctional organ, responsible for vital functions ranging from control of the endocrine system to bile secretion or vesicular trafficking, and if it is part of the liver defense system against H_2O_2.

EXPERIMENTAL PROCEDURES

Chemicals—Monoclonal anti-catalase antibody was purchased from Sigma; anti-flavoprotein of succinate ubiquinone reductase (complex II) monoclonal antibody was from Molecular Probes; anti-Bcl-2 antibody was from Santa Cruz Biotechnology; anti-PMCA was from Upstate; anti-Golgi 58K antibody was from Sigma, and anti-calreticulin was from Upstate. All other reagents were of the highest purity commercially available.

Mitochondrial Isolation and Purification—Rat liver was homogenized in isolation medium (250 mM sucrose, 5 mM Hepes, 0.5 mM EGTA, pH 7.4) and subjected to centrifugation (900 × *g*) for 5 min. The supernatant was centrifuged at 12,000 × *g* for 10 min to precipitate crude mitochondrial pellets. The pellets were resuspended in isolation medium plus 1 mM ATP and layered on top of a discontinuous gradient of Ficoll diluted in isolation medium, composed of 2-ml layers of 16 (w/v), 14, and 12% Ficoll and a 3-ml layer of 7% Ficoll. After centrifugation for 30 min at 75,000 × *g*, mitochondrial pellets were suspended in isolation medium and centrifuged again for 10 min at 12,000 × *g*. The resulting pellets were suspended in isolation medium without EGTA, and their protein content was measured by the biuret method, with bovine serum albumin as a standard. The absence of other contaminating subcellular compartments in our mitochondrial preparations has been demonstrated in previous studies (21). In addition, electron microscopy demonstrated the complete absence of contaminating membrane fragments or peroxisomes in the preparations (data not shown). It should be emphasized that the experiments with isolated rat liver mitochondria (RLM) have been performed with organelles highly purified by means of the above mentioned Ficoll gradient. The mitochondrial fraction obtained by this gradient does not exhibit any activity of urate oxidase and NADPH-cytochrome *c* reductase, peroxisomal and microsomal markers, respectively (data not shown).

Mitoplasts were obtained by hypotonic shock of mitochondria (1:10 dilution in deionized water for 5 min on ice) followed by centrifugation (10 min at 10,000 × *g*) to precipitate mitoplasts. Outer membrane and intermembrane space proteins were collected in the supernatant. MAO activity was assayed spectrophotometrically in the two fractions by monitoring the oxidation of benzylamine to benzaldehyde at 250 nm (ϵ = 12,500 M^{-1} cm^{-1}).

Subcellular Fractionation—Rat liver (250 mg) was homogenized in 1 ml of isolation medium (250 mM sucrose, 5 mM Hepes, pH 7.4) and subjected to centrifugation for 10 min at 900 × *g* (nuclei fraction, pellet I). The supernatant was then centrifuged for 1 h at 100,000 × *g* to separate cytosol from the post-nuclear particulate fraction (pellet II). The two pellets were resuspended in 1 ml of isolation medium.

Subcellular fractionation of the post-nuclear particulate fraction was performed using Optiprep™ (Accurate Chemical and Scientific Corp.). A discontinuous gradient was prepared using 30, 25, 20, 15, and 10% Optiprep™ dissolved in 50 mM Tris/HCl, pH 7.5, containing protease inhibitor mixture. The particulate fraction, resuspended in 200 μl of the above described isotonic buffer, was overlaid onto the discontinuous gradient and centrifuged at 100,000 × *g* for 3 h at 4 °C. The gradient was removed in 15 equal fractions collected from the top of the gradient. Fractions 13–15 were collected and subjected to a new discontinuous gradient (35, 30, 25, and 20 Optiprep™ dissolved in 50 mM Tris/HCl, pH 7.5, containing protease inhibitor mixture) (as described in Refs. 22, 23) and centrifuged at 100,000 × *g* for 3 h at 4 °C. 50 μl of each fraction were analyzed by Western blotting. Transferred to nitrocellulose membranes, proteins were incubated with the indicated antibody, followed by the appropriate second biotinylated antibody, and developed by means of an enhanced chemiluminescent detection system (ECL, Amersham Biosciences). Densitometric analysis of the anti-catalase spots was performed by Image Station 440 (Eastman Kodak Co.). It should be emphasized that the fractions containing RLM (6–8), of the second Optiprep™ gradient, also do not exhibit any activity by urate oxidase and NADPH-cytochrome *c* reductase, as occurs with the mitochondrial fraction obtained with the Ficoll gradient (see above) (data not shown).

Standard Incubation Procedures—Mitochondria (1 mg of protein/ml) were incubated in a water-jacketed cell at 20 °C. The standard medium contained 200 mM sucrose, 10 mM Hepes, pH 7.4, 5 mM succinate, and 1.25 μM rotenone. Variations and/or other additions are given with the individual experiments presented.

Determination of Mitochondrial Functions—Membrane potential ($\Delta\psi$) was calculated on the basis of movement of the lipid-soluble cation tetraphenylphosphonium through the inner membrane, measured on a tetraphenylphosphonium-specific electrode (24). Matrix volume was determined as reported previously (7).

Mitochondrial swelling was determined by measuring the apparent absorbance change of mitochondrial suspensions at 540 nm on a Kontron Uvikon model 922 spectrophotometer equipped with thermostatic control.

Oxygen uptake was measured by a Clark electrode. The redox state of endogenous pyridine nucleotides was followed

fluorometrically in an Aminco-Bowman 4-8202 spectrofluorometer with excitation at 354 nm and emission at 462 nm. Respiratory control index and P/O ratio were calculated as reported previously (where P/O is the ratio of the number of ATP molecules formed to the number of oxygen molecules reduced by electron transport) (14). Determination of oxidation of glutathione oxidation of glutathione was performed as described by Tietze (25).

Determination of Glutathione Peroxidase (Gpx) Activity—Gpx activity was determined by the method of Paglia and Valentine (26) in the presence of catalase inhibitors.

Determination of Urate Oxidase—Urate oxidase was determined by measuring the decrease in absorbance at 290 nm resulting from the oxidation of uric acid to allantoin. One unit oxidizes 1 μmol of uric acid per min at 25 °C in 0.1 M sodium borate buffer, pH 8.5, containing 0.1 mM uric acid (27).

Determination of NADPH-Cytochrome c Reductase—NADPH-cytochrome *c* reductase activity was assayed as described previously (28).

Assay of H_2O_2 Concentration—H_2O_2 was added to a mitochondria suspension (final concentration 0.80 mg/ml protein) in a buffer containing 10 mM Hepes, pH 7.4, with or without 15 mM ATZ, and incubated for 20 min at room temperature. The residual level of H_2O_2 in the suspension was then evaluated as reported by Angelini *et al.* (27) by adding a volume of a solution containing 4 mM 3,5-dichloro-2-hydroxybenzenesulfonic acid, 2 mM 4-aminoantipyrine, and 30 units/ml horseradish peroxidase and incubating for 15 min. The absorbance was then measured at 515 nm against a reference containing mitochondria suspension alone.

Proteinase K Treatment—Purified rat liver mitochondria was treated with 50 ng/ml proteinase K in isolation medium without EGTA (see below) with or without 0.5% Triton X-100 at room temperature for 30 min. The reaction was stopped by the addition of protease inhibitor mixture and then analyzed by Western blotting with antibodies to catalase, Bcl-2, and the flavoprotein of succinate ubiquinone reductase (complex II).

Immunogold Labeling—Isolated RLM or rat liver tissue samples were fixed for 2 h in 4% paraformaldehyde and 0.25% glutaraldehyde in 0.1 M phosphate buffer, pH 7.2, post-fixed for 1 h in 1% osmium tetroxide in the same buffer, dehydrated in ethanol, and embedded in London Resin White. Ultrathin sections picked up on gold grids were de-osmicated with sodium metaperiodate, washed with 0.01 M phosphate-buffered saline, pH 7.2, incubated for 20 min on 1% bovine serum albumin in phosphate-buffered saline, and treated with primary monoclonal antibody against catalase. After washing with phosphate-buffered saline, sections were incubated with colloidal gold (15 nm) conjugated with goat-mouse antibody. Sections were then stained with uranyl acetate followed by lead citrate and examined under the electron microscope. A control experiment was performed by eliminating the incubation of sections with the primary antibody.

RESULTS

The main problem in identifying constitutive catalase in RLM and evidencing its physiological significance on mitochondrial function is to have a mitochondrial preparation completely free of contaminant peroxisomes and other organelles. This condition was achieved by ultracentrifugation of isolated RLM on a Ficoll discontinuous gradient, as described under "Experimental Procedures." Instead, to evaluate the distribution of catalase among differing intracellular organelles, postnuclear particulate fractions were separated by ultracentrifugation on an Optiprep™ discontinuous gradient, as also described under "Experimental Procedures."

As the transit of mitochondria through a concentration gradient may cause some structural and functional damage, it is of primary importance to verify their integrity. The experiment (Fig. 1, *panel A, inset*) allows calculation of both the respiratory control index (=6) and phosphorylative capacity (ADP/O = 1.9; where ADP/O indicates mol of ADP added/mol of oxygen consumed during phosphorylation). These parameters, together the $\Delta\Psi$ value of 170 mV (Fig. 1, *panel B*), demonstrate that the organelles did not undergo any damage during purification and that they maintain optimal respiration-phosphorylation coupling.

In the presence of insufficient defense systems, oxidative stress, induced in mitochondria by ROS action, is responsible for a number of damaging effects, including membrane lipid alterations, enzyme inactivation, mutations, and mtDNA strand breaks. Indeed, at high Ca^{2+} concentrations, ROS action induces or amplifies the phenomenon of the mitochondrial permeability transition (MPT) (for reviews see Refs. 29, 30). The occurrence of the MPT is mainly characterized by colloid-osmotic swelling of the mitochondrial matrix and collapse of membrane potential ($\Delta\Psi$). The results shown in Fig. 1 reveal some effects on RLM by *tert*-butylhydroperoxide (Tbh). When treated with 100 μM Tbh, RLM incubated in standard medium, supplemented with 50 μM Ca^{2+}, exhibit an apparent absorbance decrease of the suspension of about 1 unit (Fig. 1, *panel A*). This event is accompanied by a parallel and complete drop in $\Delta\Psi$ (Fig. 1, *panel B*). The observation that cyclosporin A prevents both these effects (data not shown) indicates that the peroxide, as also observed by other authors (*e.g.* Ref. 33), induces the opening of the MPT pore. Mitochondrial swelling and $\Delta\Psi$ drop are also concomitant with almost complete oxidation of glutathione (Fig. 1, *panel C*) and oxidation of most of the pyridine nucleotides (*panel D*). All these events indicate that pore opening is closely related to oxidative stress in which the glutathione peroxidase/glutathione reductase (Gpx/Gpr) system is involved. Control determinations of Gpx activity in these RLM preparations gave a mean value of 424 ± 8.5 milliunits, in agreement with recent determinations by other authors (31).

When Tbh is substituted with the same 100 μM concentration of either hydrogen peroxide or the monoamine tyramine, the oxidation of which by mitochondrial monoamine oxidase (MAO) also generates hydrogen peroxide, none of the above mitochondrial alterations can be observed. Only at 200 μM H_2O_2 is very low oxidation of glutathione (Fig. 1, *panel C*) induced, and higher oxidation of pyridine nucleotides (Fig. 1, *panel D*), accompanied by reduced opening of the MPT pore (Fig. 1, *panel A*). Note that pyridine nucleotide oxidation is blocked after 5 min.

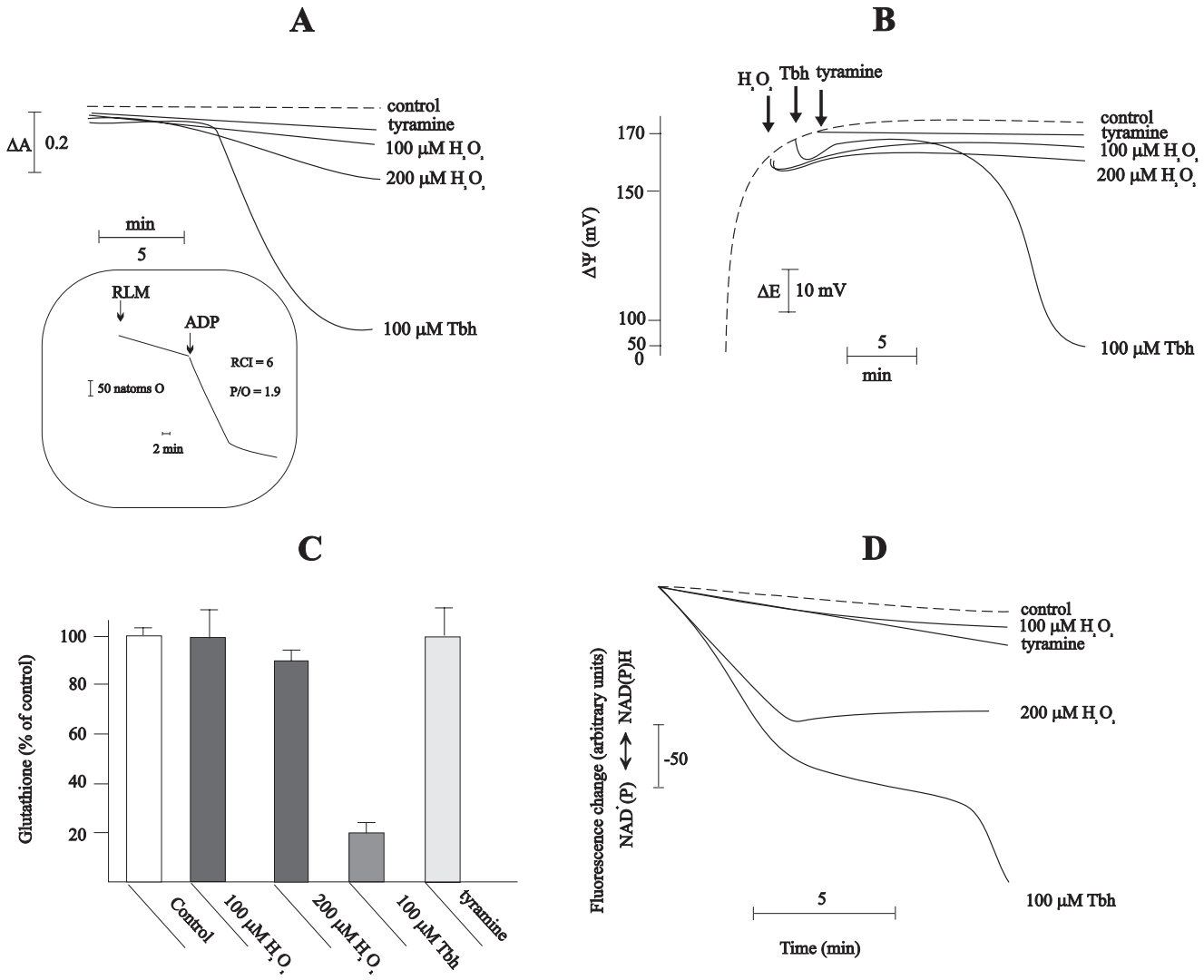

FIGURE 1. **Comparisons of effects of Tbh, H_2O_2, and tyramine in inducing membrane permeabilization (*panels A* and *B*) and oxidative stress (*panels C* and *D*) associated with MPT induction.** RLM were incubated in standard medium supplemented with 50 μM Ca^{2+} in conditions indicated under "Experimental Procedures." Tbh, H_2O_2, and tyramine were added at concentrations indicated. *A,* mitochondrial swelling. Downward deflection indicates mitochondrial swelling. *B,* membrane potential. ΔE = electrode potential. *C,* mitochondrial glutathione content. Glutathione content was measured after 15 min of incubation. *D,* pyridine nucleotide oxidation. Downward deflection indicates pyridine nucleotide oxidation. *Inset*, calculation of the respiratory control index and ADP/O. RLM were incubated in standard medium with 1 mM phosphate. Addition of 0.3 mM ADP. Assays in *panels A, B,* and *D* were performed four times with comparable results. *Panel C,* mean values ± S.D. of four experiments.

Fig. 2, *panel A,* shows that the addition of antimycin A to RLM, respiring in state 4 conditions, results in respiration block, quickly followed by a reversal of the oxygen uptake trace, indicative of O_2 generation (*trace a*). This reverse trend, as a result of O_2 production, is further augmented when 50 μM H_2O_2 is added to the incubation (Fig. 2, *trace c*). The generation of O_2 upon addition of antimycin A is completely inhibited by the catalase inhibitors aminotriazole (ATZ) or KCN (Fig. 2, *trace b*). Indeed, in the presence of the inhibitors, the respiration block because of antimycin A addition is not followed by a significant reversal of the O_2 trace after subsequent addition of H_2O_2 (Fig. 2, *trace d*).

Prompt addition of H_2O_2 to RLM at the beginning of incubation, in the absence of an energizing substrate to avoid any consumption of O_2 and production of H_2O_2, yields molecular oxygen in a 2:1 stoichiometry, *i.e.* 50 nmol of H_2O_2 generates 25 nmol of O_2, (Fig. 2, *panel B*).

Fig. 3 shows that RLM completely consume exogenously added hydrogen peroxide by a first-order reaction, with $t_{1/2}$ = 20 s. The rate of H_2O_2 consumption is not sensitive to the presence of respiratory substrates, succinate/rotenone or glutamate/malate, nor to the alkylating reagent *N*-ethylmaleimide (NEM) in concentrations known to deplete mitochondrial glutathione (Fig. 3). Instead, KCN exhibits significant inhibition with a $t_{1/2}$ = 7 min 30 s (Fig. 3). In this regard, it should be noted that pure bovine liver catalase is inhibited 95% by 200 μM KCN (results not shown). The *inset* of Fig. 3 shows the calculation of the first-order rate constant, k_0, of H_2O_2 consumption, which has a value of 0.0346 s^{-1} (r = 0.994).

The observed inefficacy in inducing serious oxidative stress and MPT induction by H_2O_2 from external sources (directly added or generated by MAO activity) (Fig. 1) and the results of experiments on O_2 generation and H_2O_2 consumption (Figs. 2 and 3) may be explained in several ways. Considering the results

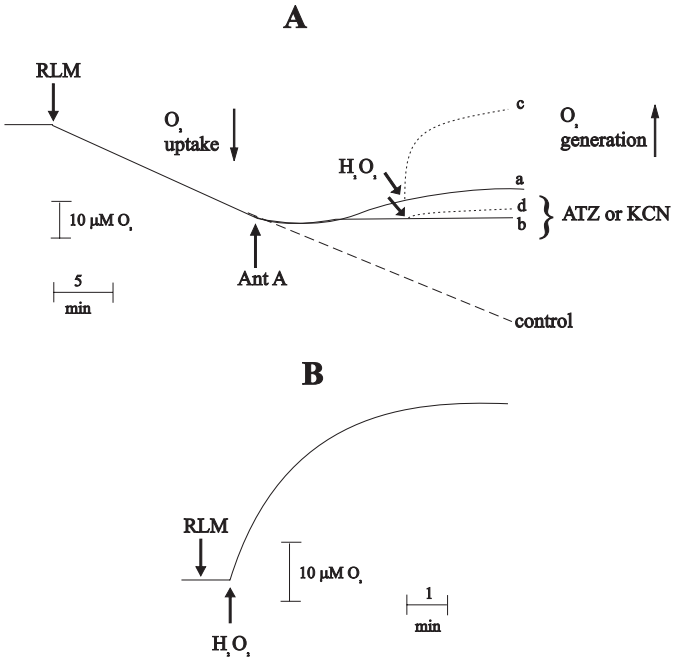

FIGURE 2. **Oxygen generation from endogenous or added H_2O_2 in isolated RLM.** *Panel A,* effect of treatment with antimycin A and ATZ or KCN (both in presence of antimycin A). RLM were incubated in standard medium, as described under "Experimental Procedures." When present in medium, ATZ and KCN were 10 μM and 200 μM, respectively. 1 μM antimycin A (*Ant. A*) and 50 μM H_2O_2 were added (see *arrows*). *Trace a,* antimycin A; *trace b,* ATZ or KCN plus antimycin A; *trace c,* antimycin A plus H_2O_2; *trace d,* ATZ or KCN plus antimycin and plus H_2O_2. Assays were performed three times with comparable results. *Panel B,* effect of exogenous H_2O_2. RLM were incubated in standard medium, deprived of succinate, in same conditions as in *panel A*. 50 μM H_2O_2 were added where indicated.

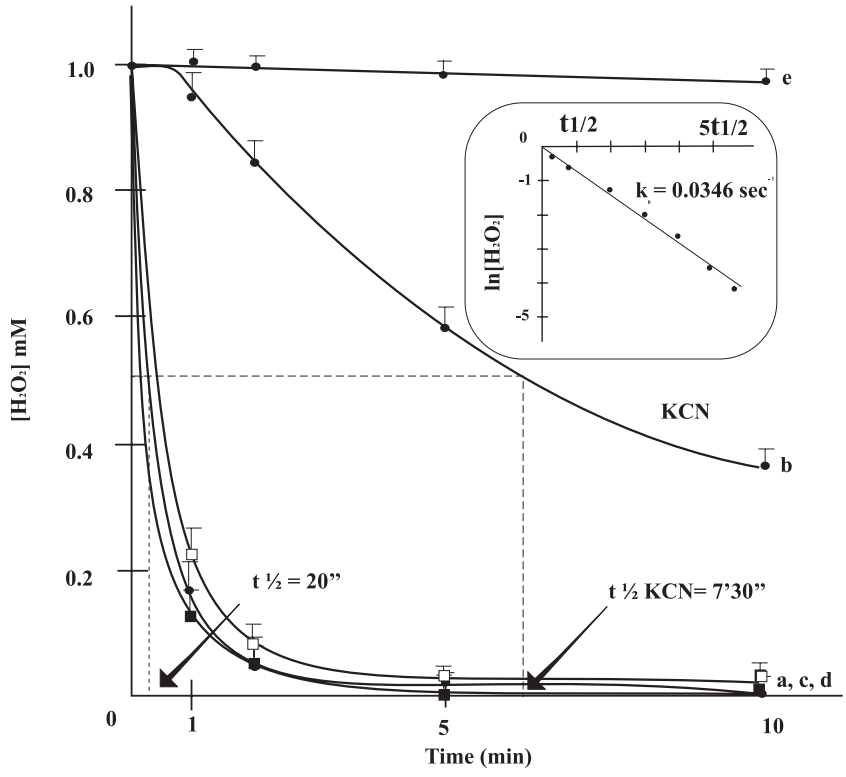

FIGURE 3. **Hydrogen peroxide consumption by isolated RLM.** RLM (0.5 mg/ml) were incubated in standard medium, in conditions described under "Experimental Procedures," with 1 mM H_2O_2 (*curve a*). When added to medium, 200 μM KCN (*curve b*), 1 mM NEM (*curve c*), succinate and 1.25 μM rotenone (*curve d*), and 5 mM glutamate and 5 mM malate (*curve d*) were present. Background H_2O_2 consumption in absence of RLM is shown in *curve e*. Data are means of four determinations. *Inset,* calculation of rate constant of catalase, k_0.

of Fig. 1 perhaps added H_2O_2 or generated by tyramine oxidation is not sufficiently transported into the matrix and is unable to induce the MPT. However, the important role of cardiolipin in favoring the diffusion of hydrogen peroxide in liposomes has already been reported (32). The effect of cardiolipin is because of the induction of stretch sensitivity in membranes made up of binary mixtures of lipids, resulting in the formation of the large voids responsible for H_2O_2 diffusion. This observation strongly suggests that this phenomenon also takes place in mitochondria.

Fig. 1 does show that 200 μM H_2O_2 has a slight or reduced effect as an oxidant (*panels C* and *D*) and MPT inducer (*panels A* and *B*), suggesting that H_2O_2 can enter the mitochondrial matrix, thus excluding the above mentioned possibility. Diffusion of H_2O_2 into the mitochondria has also been reported elsewhere (15). Perhaps RLM, although highly purified, may still be contaminated by absorption of peroxisomal or red cell-derived catalase to the outer membrane of mitochondria during liver homogenization. Indeed, catalase may also come from other subcellular compartments during the above process. Finally, RLM can contain constitutive catalase in the matrix. Our subsequent experiments were performed to verify the correct explanation between the two latter hypothesis.

Fig. 4, *panel A*, shows the distribution of catalase in various subcellular compartments obtained from homogenized liver lysate. Catalase is distributed between cytosol and particulate fraction to similar extent, whereas smaller fractions are also associated with nuclei. To observe the distribution of catalase between differing intracellular organelles, the post-nuclear particulate fractions were separated by ultracentrifugation on Optiprep™ discontinuous gradients. These fractions were Western-blotted using anti-catalase antibody and organelle-specific antibodies, including anti-plasma membrane Ca^{2+} ATP-ase (PMCA) (plasma membrane), anti-Golgi 58K (Golgi complex), anti-calreticulin (endoplasmic reticulum), anti-cathepsin D (lysosomes), and anti-flavoprotein of complex II (mitochondria). The plasma membrane was present in the lighter fractions 1–2. The Golgi complex was distributed between fractions 5 and 7. Endoplasmic reticulum was present in fractions 8–12, lysosomes in fractions 9–12, and mitochondria in fractions 13–15 (Fig. 4, *panel B*). The results clearly show that there are peaks of catalase corresponding to all subcellular markers, demonstrating that it is associated with various intracellular compartments, including mitochondria. However, peroxisomes may copurify with

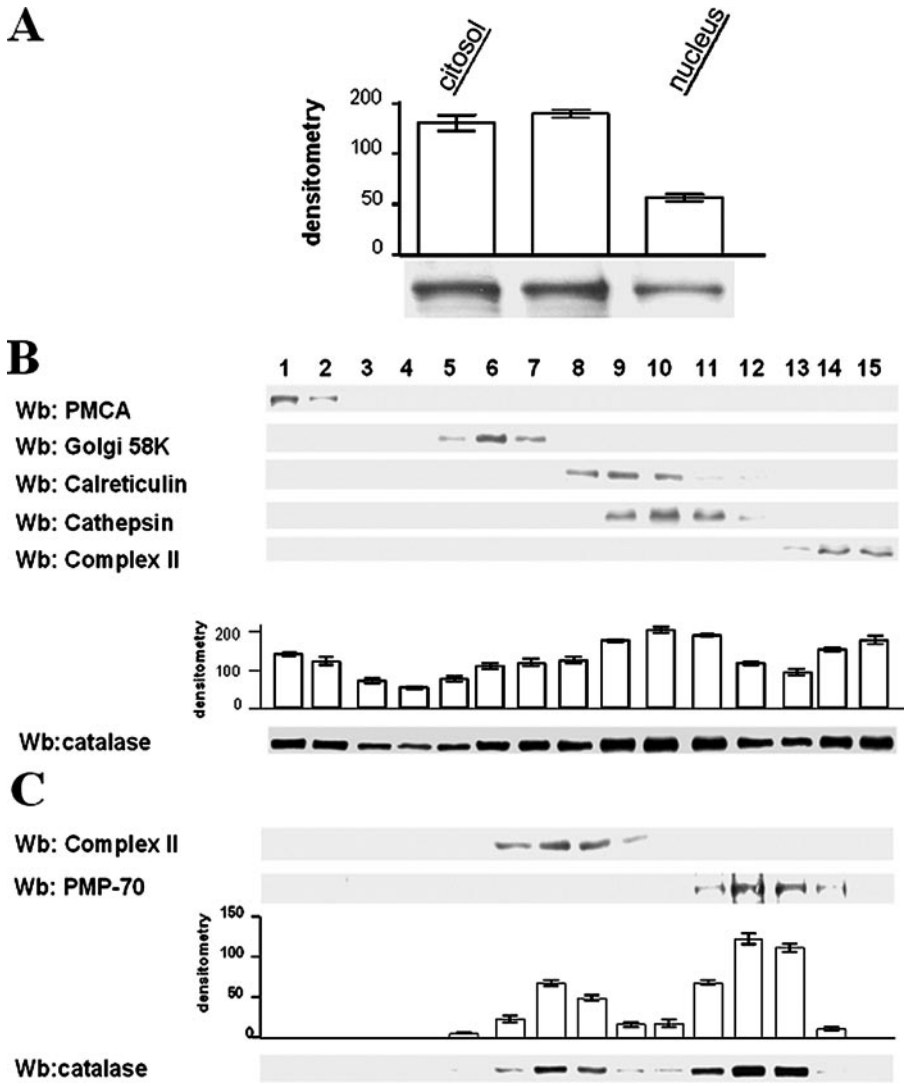

FIGURE 4. **Subcellular fractionation of homogenized liver lysate.** *Panel A,* aliquots of cytosol, post-nuclear particulate, and nuclei were analyzed by Western blotting with antibody anti-catalase. *Panel B,* post-nuclear particulate fraction was centrifuged at discontinuous Optiprep™ gradients, as described under "Experimental Procedures," and aliquots of resulting fractions were analyzed by Western blotting (*Wb*) with anti-PMCA antibodies (plasma membrane), anti-Golgi 58K (Golgi complex), anti-calreticulin (endoplasmic reticulum), anti-cathepsin (lysosomes), anti-flavoprotein of complex II (mitochondria), and anti-catalase. *Panel C,* fractions 13–15 were collected and centrifuged at a new discontinuous Optiprep™ gradient, as described under "Experimental Procedures," and aliquots of resulting fractions were analyzed by Western blotting with anti-flavoprotein of complex II (mitochondria), anti-PMP70 (peroxisomes), and anti-catalase. The amount of particulate fractions was ¼ of those used in *panel B*, to avoid the saturation of the Western blot. Mean of densitometric amount of catalase is reported *above* relative spots.

mitochondria (results not shown). To separate mitochondria from peroxisomes, fractions 13–15 were collected and separated by ultracentrifugation on a new Optiprep™ discontinuous gradient as described in Refs. 22, 23 (see "Experimental Procedures"). These new fractions were Western-blotted using anti-catalase, anti-PMP70 (peroxisomes), and anti-flavoprotein of complex II (mitochondria) antibodies (Fig. 4, *panel C*). This new gradient, made up with a reduced amount of the sample (¼) when compared with that of Fig. 4, *panel B*, separates mitochondria from peroxisomes and shows that a specific catalase peak is also associated with the mitochondrial fraction (Fig. 4, *panel C*), although its expression is lower than that of the peroxisomal fraction. As also reported under "Experimental Procedures," it should be noted that this mitochondrial fraction corresponds to that obtained by the Ficoll gradient.

If the presence of catalase in mitochondria is well documented by the above results, it is not yet clear if the enzyme is constitutively present in the inner compartments or, as above mentioned, it comes from peroxisomes or other organelles and is absorbed with the outer membrane of mitochondria. To distinguish between these two possibilities, we fractionated purified RLM into fraction A (mitoplasts) and fraction B (outer membrane plus intermembrane space) and determined MAO activity in all fractions (Fig. 5, *panel A*). Contemporaneously, intact RLM and fractions A and B, maintaining the same ratio between the two subcompartments, were submitted to SDS-PAGE and Western blotting with antibody anti-catalase (Fig. 5, *panel A*). The results show that maximum MAO activity and the higher presence of catalase are detected in intact RLM. However, very large amounts of catalase are also detected in mitoplasts (fraction A), in which MAO activity is obviously very low, whereas fraction B has a very small amount of catalase, indicating that catalase is mainly located in the inner mitochondrial compartment. Note that in both fractions A and B, as observed in intact RLM (see "Experimental Procedures"), the activity of urate oxidase and NADPH-cytochrome *c* reductase is almost completely absent (data not shown), further demonstrating, together with the bioenergetic parameters (Fig. 1, *panel A*, *inset*, and *panel B*), the purity and the integrity of mitochondrial preparations. We also assessed the sensitivity of mitochondria-associated catalase to proteinase K. Intact RLM were incubated with proteinase K with or without Triton X-100, and mitochondrial proteins were Western-blotted for catalase, Bcl-2, and flavoprotein of complex II. As shown in Fig. 5, *panel B*, flavoprotein of complex II, which is located inside mitochondria at the level of the inner membrane, was fully protected from proteinase K in the absence of detergent, whereas Bcl-2, which is peripherally associated with the external mitochondrial membrane, was completely degraded, regardless of whether Triton X-100 was added or not. Catalase was not degraded by proteinase K with-

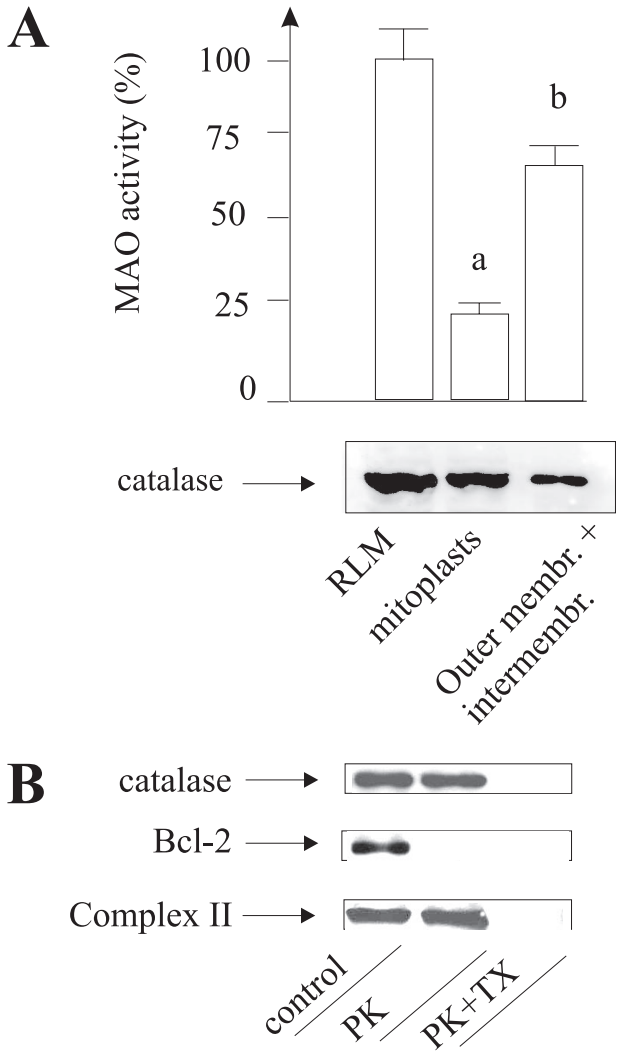

FIGURE 5. **Catalase detection in submitochondrial fractions.** *Panel A,* RLM were subfractionated as described under "Experimental Procedures" in mitoplasts (*fraction a*) and outer membrane plus intermembrane space (*fraction b*). Fractions were analyzed for MAO activity (reported as percentage of control) and, in presence of catalase, by Western blotting with anti-catalase antibody. *Panel B,* intact RLM were treated with 50 ng/ml proteinase K (*PK*) with or without 0.5% Triton X-100 (*TX*) at room temperature for 30 min. Reaction was analyzed by Western blotting with antibodies anti-catalase, -Bcl-2, and -flavoprotein of complex II. Results in histogram are the mean values ± S.D. of four experiments. Western blots report typical experiments. 3 other experiments of both the panels gave almost identical spots.

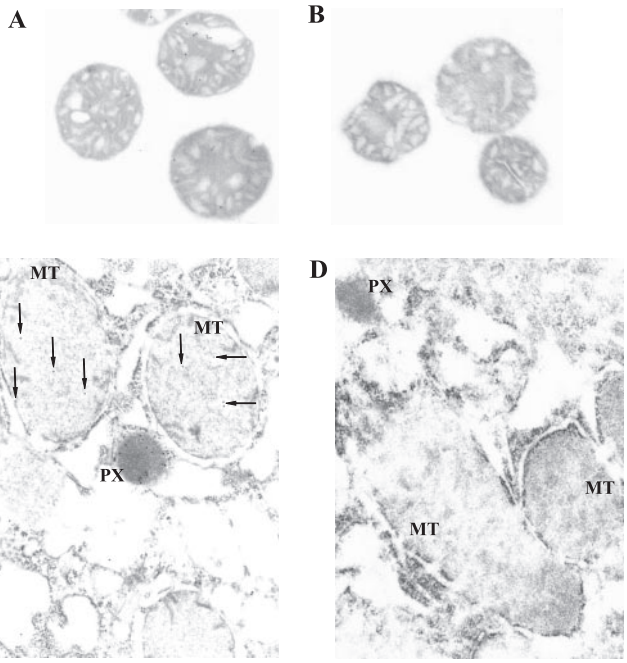

FIGURE 6. **Immunogold detection of catalase in isolated RLM and whole liver tissue.** *Panel A,* section of isolated rat liver mitochondria incubated with catalase antibody, followed by gold-conjugated secondary antibody. *Panel B,* negative control, in which gold-labeled secondary antibody was added without catalase antibody. *Panel C,* section of rat liver incubated with catalase antibody, followed by gold-conjugated secondary antibody. *Arrows,* mitochondrial labeling by gold particle. *Panel D,* negative control, in which gold-labeled secondary antibody was added without catalane antibody. *MT,* mitochondria; *PX,* peroxisomes. Detection of isolated RLM and whole tissue from liver of five animals gave similar results.

out Triton X-100, indicating that it is mainly located inside mitochondria (Fig. 5, *panel B*). To further define catalase location within mitochondria, immunogold staining on isolated RLM (Fig. 6, *panels A* and *B*) and whole rat liver tissue (Fig. 6, *panels C* and *D*) was performed, allowing direct visual location of catalase in mitochondria. Isolated RLM and rat liver tissue were probed with an anti-catalase primary antibody and a gold particle-conjugated anti-mouse secondary antibody. Isolated mitochondria (Fig. 6, *panel A*) and mitochondria in rat liver tissue (MT) (Fig. 6, *panel B*) are clearly labeled. No background staining was seen with secondary antibody alone (Fig. 6, *panels B* and *D*). Fig. 6, *panel A*, shows that all gold particles were found in matrix space. Immunogold experiments on whole rat liver tissue (Fig. 6, *panel B*), confirming intramitochondrial labeling, exclude the possibility that the observed mitochondrial location is the consequence of migration from other subcellular compartments during the isolation procedure.

DISCUSSION

The results reported here for the first time bring compelling evidence that catalase is present inside liver mitochondria and also that it takes part in the oxidative stress defense.

Experiments on oxygen generation by endogenous or exogenous catalase (Fig. 2, *panels A* and *B*) and hydrogen peroxide consumption by highly purified RLM (Fig. 3) clearly indicated the presence of catalase in RLM, with an activity of 825 ± 15 units (Fig. 3). One unit of enzyme activity represents 1 μM of substrate consumed per min. Indeed, taking into account previous calculations of k_0 on highly purified liver catalase (34), it may be inferred that mitochondrial catalase has approximately a concentration of 14×10^{-4} μM and taking into account a matrix volume of 1.2 μl/mg protein, a turnover number (molecular activity) of 1.6×10^7 s^{-1}, in agreement with previous calculations (*e.g.* see ref. 35). The observed first-order reaction of H_2O_2 decomposition, accompanied by O_2 release with a reaction stoichiometry of 2:1, is indicative of a catalatic rather than a peroxidatic mechanism for catalase activity (17, 36). As reported previously, cytochrome *c* oxidase has a weak catalase-like activity in the oxidized (ferric) form but not in the reduced (ferrous) form (37), so that this complex may co-participate in the removal of H_2O_2. However, addition of the respiratory substrates succinate and glutamate plus malate, which reduce cytochrome *c* oxidase, do not induce any inhibition on the decom-

position of hydrogen peroxide (Fig. 3). This observation indicates that complex IV of the respiratory chain is not involved in the observed decomposition.

The constitutive presence of catalase in RLM is definitively confirmed by subcellular and submitochondrial fractionating analyses and immunogold detections. The results shown in Fig. 4 show that subcellular fractions, obtained by ultracentrifugation on an Optiprep™ discontinuous gradient, have catalase peaks associated with all intracellular organelles, including mitochondria (Fig. 4, *panels A* and *B*). A further analysis of mitochondrial fractions using markers for mitochondria and peroxisomes clearly distinguished catalase associated with mitochondria and peroxisomes (Fig. 4, *panel C*). Indeed, as demonstrated by the results of Fig. 5, mitochondrial catalase is mainly located in the mitochondrial matrix. Immunogold electron microscopy of isolated RLM clearly confirms the presence of catalase in the inner mitochondrial compartments (Fig. 6, *panel A*). The same type of experiment performed on liver tissue (Fig. 6, *panel B*) unequivocally demonstrates the presence of constitutive catalase in "*in situ*" mitochondria.

The above conclusion is also supported by Zeng and co-workers (38) who applied a high-throughput comparative proteome experimental strategy between RLM prepared with traditional centrifugation (CM) and further purified with Nycodenz gradient (PM). A ratio of PM:CM >1 is predictive of mitochondrial location, and catalase has a ratio of >1 (38).

It should be noted that catalase is able to exhibit its action up to a threshold concentration of H_2O_2, most probably between 100 and 200 μM. Higher concentrations induce some oxidation and, consequently, a slight induction of MPT (Fig. 1). The amount of pyridine nucleotides oxidized by 200 μM H_2O_2 (Fig. 1, *panel D*) is most probably part of a pool located in the external compartments of RLM. This oxidation is most probably because of hydrogen peroxide (or the derived hydroxyl radical) before its complete removal by matrix catalase.

Constitutive catalase, alone, can completely remove exogenously added H_2O_2 (Fig. 3). In fact, depletion of glutathione by NEM does not alter the rate of H_2O_2 breakdown (Fig. 3), demonstrating that the Gpx/glutathione reductase system is not involved in H_2O_2 removal. The partial oxidation of glutathione and pyridine nucleotides and the consequent low amplitude swelling induced by very high exogenous concentrations of H_2O_2 (Fig. 1) are most probably because of the generation of hydroxyl radical (see below), which precedes the complete scavenging of H_2O_2.

In conclusion, depending on its possible transformation into hydroxyl radical, despite the very high turnover number of catalase, H_2O_2 is dose-dependent on its effects. It should also be pointed out that matrix catalase can eliminate overproduction of hydrogen peroxide by RLM when treated with isoflavones (9), cyclic terpenes (10), salicylate (15), etc. In this regard, we emphasize that part of the H_2O_2 formed as a result of the interaction of these drugs with the respiratory chain is rapidly transformed into the hydroxyl radical (Fenton reaction). The transition metal necessary for this reaction, a Fe^{2+} belonging to some iron-sulfur center or cytochrome of mitochondrial complexes, is very close to the site of H_2O_2 generation (*i.e.* N-2 center of complex I (11) or the cytochrome b_H heme of complex III) (9). The highly reactive $OH^{\bullet}$ oxidizes critical thiol groups located on the translocase of adenine nucleotides (39), which results in pore opening (see above). Instead, the residual H_2O_2 is scavenged by mitochondrial catalase and the Gpx/glutathione reductase system. On one hand, these observations highlight the detoxifying effect of constitutive mitochondrial catalase against overproduction of hydrogen peroxide and on the other hand the physiopathological role of H_2O_2 generated by RLM upon interaction with pro-oxidant agents, with the induction of MPT and, potentially, the triggering of apoptosis.

In conclusion, hydrogen peroxide released by mitochondria reflects the steady-state concentration of H_2O_2 dependent on the rate of its generation by the respiratory chain, its transformation into hydroxyl radical, and its decomposition by matrix catalase. However, it should also be recalled that the capacity of catalase to decompose H_2O_2 may depend on the location of the enzyme and the site of H_2O_2 generation. For quantitative measurements of hydrogen peroxide in intact mitochondria, besides these considerations, it should be noted that the detection system operates outside the mitochondria, which means that the measured amount is that which is able to flow from the organelles before undergoing the above mentioned transformation and decomposition.

It should also be emphasized that if the catalase of RLM has a strategic location like that of heart mitochondria, *i.e.* near the primary loci of H_2O_2 generation (see above), then catalase activity may control the amount of H_2O_2 engaged in interactions with the respiratory chain to produce hydroxyl radical and consequently to induce the MPT. In this regard, analysis of electron chain complexes and Krebs cycle enzymes in heart mitochondria revealed inactivation of succinate dehydrogenase, α-ketoglutarate dehydrogenase, and aconitase by H_2O_2 (40). The presence of constitutive catalase in RLM may also represent a regulatory control on the activity of the Krebs cycle, respiratory chain, and ATP synthesis. As reported previously (12), the antioxidant efficacy of mitochondrial catalase, when evaluated at cellular level, may depend on the type of oxidative agent and the site of ROS production. In fact, if mitochondrial catalase can protect the organelles against oxidative stress and MPT, and potentially protects cells against apoptosis induced by exogenous or endogenous H_2O_2, this enzyme may enhance the sensitivity of cells to apoptosis induced by the toxin TNF-α (15).

The presence in liver of mitochondrial catalase and the above mentioned effect on TNF-α activity may have important implications. It has been reported that liver injury induced by TNF-α, but also liver regeneration and hepatocarcinogenesis, are causatively linked to the activation of particular pathways, including ROS generation. These pathways interact with each other to regulate hepatocyte apoptosis and proliferation (41). Taking into account these observations and considering that mitochondrial catalase efficiently removes the H_2O_2 produced by TNF-α (15) by its interaction with mitochondrial complex I (42), effectors of activity and expression of mitochondrial catalase may be new tools for the treatment of hepatitis and hepatocarcinoma.

Acknowledgment—We thank Mario Mancon who was involved in technical support of this work.

REFERENCES

1. Finkel, T., and Holbrook, N. J. (2000) *Nature* **408,** 239–247
2. Afanas'ev, I. B. (2005) *Biogerontology* **6,** 283–290
3. Tappel, A. L. (1973) *Fed. Proc.* **32,** 1870–1874
4. Zamzami, N., Susin, S. A., Marchetti, P., Hirsch, T., Gomez-Monterrey, I., Castedo, M., and Kroemer, G. (1996) *J. Exp. Med.* **183,** 1533–1544
5. Freeman, B. A., and Crapo, J. D. (1982) *Lab. Investig.* **47,** 412–426
6. Davies, K. J., and Doroshow, J. H. (1986) *J. Biol. Chem.* **261,** 3060–3067
7. Marcocci, L., De Marchi, U., Salvi, M., Micella, Z. G., Nocera, S., Agostinelli, E., Mondovi, B., and Toninello, A. (2002) *J. Membr. Biol.* **188,** 23–31
8. Hodnick, W. F., Milosavljevic, E. B., Nelson, J. H., and Pardini, R. S. (1998) *Biochem. Pharmacol.* **37,** 2607–2611
9. Salvi, M., Brunati, A. M., Clari, G., and Toninello, A. (2002) *Biochim. Biophys. Acta* **1556,** 187–196
10. Salvi, M., Fiore, C., Armanini, D., and Toninello, A. (2003) *Biochem. Pharmacol.* **66,** 2375–2379
11. Fiore, C., Salvi, M., Palermo, M., Sinigaglia, G., Armanini, D., and Toninello, A. (2004) *Biochim. Biophys. Acta* **1658,** 195–201
12. Kowaltowski, A. J., and Vercesi, A. E. (1999) *Free Radic. Biol. Med.* **26,** 463–471
13. Salvi, M., Fiore, C., Battaglia, V., Palermo, M., Armanini, D., and Toninello, A. (2005) *Endocrinology* **146,** 2306–2312
14. Battaglia, V., Salvi, M., and Toninello, A. (2005) *J. Biol. Chem.* **280,** 33864–33872
15. Bai, J., and Cederbaum, A. I. (2001) *Biol. Signals Recept.* **10,** 189–199
16. Neubert, D., Wojtczak, A. B., and Lehninger, A. L. (1962) *Proc. Natl. Acad. Sci. U. S. A.* **48,** 1651–1658
17. Radi, R., Turrens, J. F., Chang, L. Y., Bush, K. M., Crapo, J. D., and Freeman, B. A. (1991) *J. Biol. Chem.* **266,** 22028–22034
18. Petrova, V. Y., Drescher, D., Kujumdzieva, A. V., and Schmitt, M. J. (2004) *Biochem. J.* **380,** 393–400
19. Arita, Y., Harkness, S. H., Kazzaz, J. A., Koo, H. C., Joseph, A., Melendez, J. A., Davis, J. M., Chander, A., and Li, Y. (2005) *Am. J. Physiol.* **290,** L978–L986
20. Schriner, S. E., Linford, N. J., Martin, G. M., Treuting, P., Ogburn, C. E., Emond, M., Coskun, P. E., Ladiges, W., Wolf, N., Van Remmen, H., Wallace, D. C., and Rabinovitch, P. S. (2005) *Science* **308,** 1909–1911
21. Salvi, M., Brunati, A. M., Bordin, L., La Rocca, N., Clari, G., and Toninello, A. (2002) *Biochim. Biophys. Acta* **1589,** 181–195
22. Joly, E., Bendayan, M., Roduit, R., Saha, A. K., Ruderman, N. B., and Prentki, M. (2005) *FEBS Lett.* **579,** 6581–6586
23. Van Veldhoven, P. P., Baumgart, E., and Mannaerts, G. P. (1996) *Anal. Biochem.* **237,** 17–23
24. Kamo, N., Muratsugu, M., Hongoh, R., and Kobatake, Y. (1979) *J. Membr. Biol.* **49,** 105–121
25. Tietze, F. (1969) *Anal. Biochem.* **27,** 502–522
26. Paglia, D. E., and Valentine, W. N. (1967) *J. Lab. Clin. Med.* **70,** 158–169
27. Angelini, R., Rea, G., Federico, R., and D'Ovidio, R. (1996) *Plant Sci.* **119,** 103–113
28. Sottocasa, G. L., Kuylenstierna, B., Ernster, L., and Bergstrand, A. (1967) *J. Cell Biol.* **32,** 415–438
29. Kim, J. S., He, L., and Lemasters, J. J. (2003) *Biochem. Biophys. Res. Commun.* **304,** 463–470
30. Toninello, A., Salvi, M., and Mondovi, B. (2004) *Curr. Med. Chem.* **11,** 2349–2374
31. Schild, L., Plumeyer, F., and Reiser, G. (2005) *FEBS J.* **272,** 5844–5852
32. Mathai, J. C., and Sitaramam, V. (1994) *J. Biol. Chem.* **269,** 17784–17793
33. Nieminen, A. L., Byrne, A. M., Herman, B., and Lemasters, J. J. (1997) *Am. J. Physiol.* **272,** C1286–C1294
34. Greenfield, R. E., and Price, V. E. (1954) *J. Biol. Chem.* **209,** 355–361
35. Nicholls, P., Loewen, P., and Fita, I. (2001) *Adv. Inorg. Chem.* **51,** 52–106
36. Chance, B., Sies, H., and Boveris, A. (1979) *Physiol. Rev.* **59,** 527–605
37. Orii, Y. (1982) *J. Biol. Chem.* **257,** 9246–9248
38. Jiang, X. S., Dai, J., Sheng, Q. H., Zhang, L., Xia, Q. C., Wu, J. R., and Zeng, R. (2005) *Mol. Cell. Proteomics* **4,** 12–34
39. Costantini, P., Belzacq, A. S., Vieira, H. L., Larochette, N., De Pablo, M. A., Zamzami, N., Susin, S. A., Brenner, C., and Kroemer, G. (2000) *Oncogene* **19,** 307–314
40. Nulton-Persson, A. C., and Szweda, L. I. (2001) *J. Biol. Chem.* **276,** 23357–23361
41. Schwabe, R. F., and Brenner, D. A. (2006) *Am. J. Physiol.* **290,** G583–G589
42. Goossens, V., Stange, G., Moens, K., Pipeleers, D., and Grooten, J. (1999) *Antioxid. Redox. Signal.* **1,** 285–295

Catalase Takes Part in Rat Liver Mitochondria Oxidative Stress Defense

Mauro Salvi, Valentina Battaglia, Anna Maria Brunati, Nicoletta La Rocca, Elena Tibaldi, Paola Pietrangeli, Lucia Marcocci, Bruno Mondovì, Carlo A. Rossi and Antonio Toninello

J. Biol. Chem. 2007, 282:24407-24415.
doi: 10.1074/jbc.M701589200 originally published online June 18, 2007
